Article

UDC 538.9; 535.215; 539.23; 535.3
https://doi.org/10.31489/2025PH3/6-15

Received: 21.04.2025
Accepted: 23.06.2025

A.K. Mussabekova[1]✉, A.K. Aimukhanov[1], A.K. Zeinidenov[1],
A.Z. Ziyat[1], K.T. Abdrakhman[1], A.M. Alexeev[2]

[1]*Buketov University, Scientific Center of nanotechnology and functional nanomaterials, Karaganda, Kazakhstan;*
[2]*Kazan Federal University, Kazan, Russia*

The Influence of Al_2O_3 Nanoparticles on Electron Transport in a Polymer Solar Cell

The effect of Al_2O_3 nanoparticles on the electron transport of SnO_2-based electron transport layer (ETL) in polymer solar cells was studied. Comprehensive studies of the morphology, optical, electrophysical and photoelectric properties of the composite films were carried out. It was found that doping SnO_2 films with Al_2O_3 nanoparticles leads to a decrease in the surface roughness of the composite films. According to the absorption spectra, it was shown that an increase in the concentration of Al_2O_3 nanoparticles in SnO_2 films leads to a decrease in the optical bandgap. Analysis of the impedance spectra showed that there is a critical concentration of Al_2O_3 nanoparticles at which the maximum improvement in the electrotransport characteristics of SnO_2 films is observed. At high Al_2O_3 concentrations (over 15 %), a decrease in electron mobility and an increase in recombination in the studied composite film are observed. Photovoltaic measurements have demonstrated that the highest efficiency of 2.8 % polymer solar cells is achieved at an optimal concentration of Al_2O_3 nanoparticles equal to 15 %. Further increase in the content of Al_2O_3 nanoparticles leads to a decrease in the efficiency of polymer solar cells. Since localized negative charges in Al_2O_3 nanoparticles create a local electric field, they screen the recombination of minority charge carriers in ETL SnO_2. This suppresses the leakage current in devices. Therefore, it is important to investigate the charge transfer mechanism in SnO_2:Al_2O_3 films and evaluate their potential for application in polymer solar cells.

Keywords: SnO_2, Al_2O_3, morphology, absorption, band gap, Bode plots, impedance, current-voltage characteristics

✉*Corresponding author*: Assel K. Mussabekova, assel50193@gmail.com

Introduction

The demand for transparent conductive oxides (TCO) materials that combine high optical transparency and good electrical conductivity is growing rapidly due to the development of optoelectronic technologies. Such materials are in demand in thin-film solar cells [1], charge storage devices [2], flat-panel displays [3], gas sensors [4] and other applications. The most studied TCOs are films based on TiO_2, ZnO, SnO_2 and others, research that has been ongoing for over 40 years. These materials are wide-bandgap n-type semiconductors. Among the known n-type TCOs, the best characteristics are demonstrated by In_2O_3:Sn, SnO_2:F and ZnO:Al composites [5], which have a transparency above 90 % and a specific resistance of about 10^{-4} Ohm·cm [6, 7].

SnO_2 and its composite materials are widely known for their pronounced structural and optical properties when scaled down to the nanoscale. The efficiency of devices based on them is largely determined by the electrical and optical properties of transparent electrodes, as well as the technology of their production [8]. It is known that the degree of improvement of these properties depends significantly on the chemical composition, particle size and specific surface area of SnO_2.

One of the major challenges in obtaining high-performance SnO_2-based organic solar cells (OSCs) is the presence of defects such as oxygen vacancy [9] and other surface-related defects [10, 11]. These can lead to poor charge transport and low power conversion efficiency (PCE) in devices [12]. In addition, oxygen-induced degradation of the photoactive layer can occur in the metal oxide layer, allowing atmospheric oxygen to diffuse into the cell, resulting in an increase in defects that adversely affect the performance of the device [13]. Minimizing defects and reducing carrier recombination in the SnO_2 film by passivating the ETL/photoactive layer interface is critical in the fabrication of high-performance OSCs.

Wu et al. reported that the defect states of ZnO were suppressed by modifying its surface with an ultrathin Al layer, which could be partially oxidized to AlO_x [14]. It is known that the ultrathin Al_2O_3 film is an effective surface passivation method in silicon-based solar cells by utilizing its unique ability to form a layer without point defects [15]. It not only provides good chemical passivation by reducing the defect density at the interface through the hydrogen passivation associated with the deposition process, but also leads to a decrease in the minority carrier concentration near the interface due to the built-in electric field, which is called field effect passivation [16, 17]. In this case, the negative charges localized in the Al_2O_3 layer create a local electric field that screens the recombination of minority carriers [18]. Moreover, it is reported that the Al_2O_3 layer can also suppress the leakage current in the device, which turns out to be another advantage of Al_2O_3 passivation [19]. Currently, Al_2O_3 composites are at the threshold of commercial solar cell production and large-scale photovoltaic cell production [20], while there are rare reports of their use for OSC passivation. Thus, the use of Al_2O_3 may have potential applications in the field of photovoltaics.

Despite the studies conducted on the synthesis of SnO_2 films doped with Al_2O_3 [21], their electrotransport properties are still poorly understood. Therefore, it is important to study the charge transfer mechanism in such films and evaluate their potential for use in optoelectronic devices. This paper presents the results of a study of the effect of Al_2O_3 nanoparticles on electron transport in ETL SnO_2 polymer solar cells.

Experimental

Thin films preparation

The preparation of FTO substrates was carried out according to the procedure detailed in reference [22]. Composite films based on SnO_2 were obtained by the sol-gel method. The scheme for preparing composite films is shown in Figure 1. The initial reagents were $SnCl_2$ (99.9 %, Sigma Aldrich) in an amount of 2.25 g and $AlCl_3$ (99.9 %, Sigma Aldrich) in an amount corresponding to Al_2O_3 concentrations of 5 % (0.0667 g), 10 % (0.1334 g), 15 % (0.2001 g), 20 % (0.2268 g) and 25 % (0.33335 g). $SnCl_2$ and Al_2O_3 were dissolved in 1 ml of ethyl alcohol (99.9 %, Sigma Aldrich).

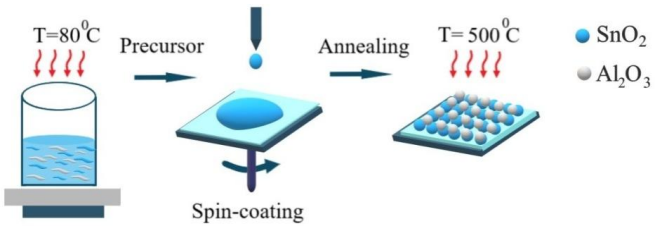

Figure 1. Scheme for preparing SnO_2:Al_2O_3 composite films

Afterwards, the prepared solutions were continuously stirred at 80 °C for 2 hours, followed by 24 hours at room temperature to complete the reactions and composition. Then, the obtained solution was applied to the surface of the substrates by centrifugation (on a SPIN150i centrifuge, Semiconductor Production System) at a rotation speed of 4000 rpm. The rotation time of the centrifuge at this rotation speed was 30 seconds. The obtained films were thermally annealed in air at a temperature of 500 °C for 1 hour.

To assemble the FTO/SnO_2:Al_2O_3/P3HT:PCBM/PEDOT:PSS/AgOSC, the photoactive material P3HT:PCBM was dissolved in chlorobenzene and stirred for 24 hours at room temperature. The photoactive layer was applied by centrifugation at a rotation speed of 2000 rpm on the FTO substrate, previously

deposited with the SnO_2:Al_2O_3 film. Afterwards, the obtained film was annealed in air at a temperature of 140 °C. The hole-transport layer of PEDOT:PSS was applied to the surface of the photoactive layer at a substrate rotation speed of 3000 rpm, after which the substrate was annealed at a temperature of 120 °C. At the final stage of OSC assembly, a silver electrode was applied to the surface of the hole-transport layer by vacuum-thermal deposition.

Analysis methods

Film surface morphology images were obtained using a MIRA 3LMU (TESCAN) electron microscope. A Co sample (9905-17, Micro-Analysis Consultants Ltd Unit 19, Edison Road, St lves Cambridgeshire PE27 3 LF U.K.) was used as a standard for EDX analysis. The surface topography of the samples was studied using a JSPM–5400 atomic force microscope manufactured by JEOL Ltd. Probes manufactured by NT-MDT were used for scanning. Scanning was performed in a semi-contact mode with resonance frequency parameters of 140–390 kHz, cantilever stiffness of 3.1–37.6 N/m, and probe rounding radius of 10 nm; the scanning speed was 10 μm/s. Surface morphology parameters were calculated using the WinspmII Data Processing software package manufactured by JEOL Ltd.

The absorption spectra of the films were measured using the Avantes universal spectrometric complex based on the AvaSpec-ULS2048CL-EVO spectrometer and the AvaLight-DHc deuterium-halogen combined light source with a spectral emission range of 200–2500 nm.

The current-voltage characteristics of the solar cells were measured using the PVIV-1A setup (Newport. Canada). The Sol3A solar energy simulator (class AAA, Newport. Canada) with a radiation intensity of 100 mW/cm^2 was used as a light source.

The impedance spectra were measured using a P-45X potentiostat-galvanostat (Elins, Russia) with an additional FRA-24M frequency analyzer module installed to measure the electrophysical characteristics on alternating current.

Results and Discussion

Surface morphology

Figure 2 shows scanning electron microscope (SEM) images of the surface morphology of SnO_2 and SnO_2:Al_2O_3 (25 %) films, as well as a cross-section of the films. Analysis of the SEM images demonstrates the presence of micro-holes on the surface of the SnO_2 films, which is typical for thin-film structures [23]. Comparison of SnO_2:Al_2O_3 films with different concentrations of Al_2O_3 shows that the addition of 25 % Al_2O_3 to SnO_2 leads to the formation of a more uniform surface structure: the films become smoother and fine-grained, indicating a change in morphology when doped with Al_2O_3 nanoparticles.

Cross-section images of the studied films demonstrate that the film thickness increases with the addition of Al_2O_3 nanoparticles to SnO_2 from 79.69 nm to 93.73 nm.

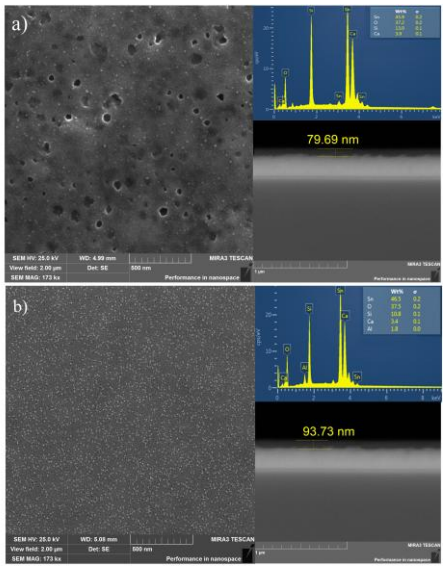

Figure 2. SEM images of the morphology of films and cross-section of SnO_2, SnO_2:Al_2O_3 (25 %). Inset shows EDX spectra

Figure 3 shows atomic force microscope (AFM) images of SnO_2 and SnO_2:Al_2O_3 (25 %) films. The root mean square roughness (RMS) values for SnO_2 and SnO_2:Al_2O_3 (25 %) films are 2.4 and 1.83, respectively.

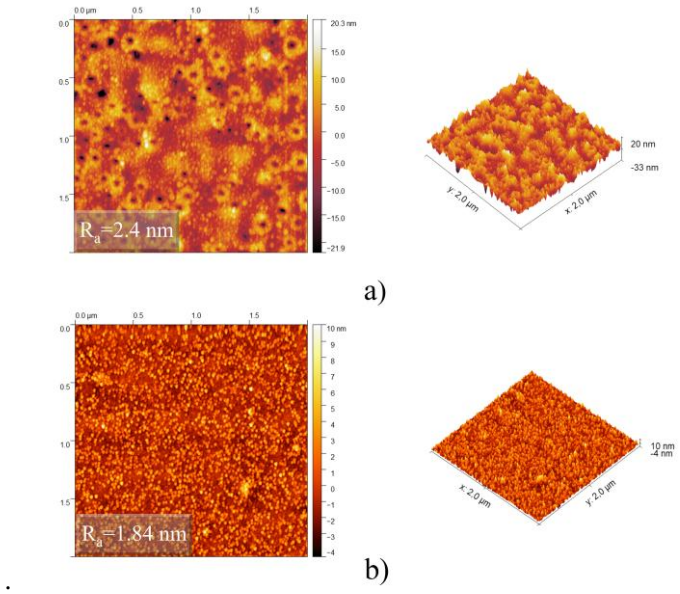

Figure 3. AFM images of SnO_2 and SnO_2:Al_2O_3 (25 %) films

From the analysis of the surface morphology it follows that the addition of Al_2O_3 helps to reduce the roughness of the films. This phenomenon can be explained by the fact that Al_2O_3 helps to reduce and fill the micro-holes present on the surface of SnO_2 films, thereby improving the texture and increasing the homogeneity of the surface.

Optical properties

Figure 4*a* shows the absorption spectra of SnO_2 films and SnO_2:Al_2O_3 composite films with different concentrations of Al_2O_3 nanoparticles (5 %, 10 %, 15 %, 20 %, 25 %). It follows from the analysis of the spectra that all the studied samples have a relatively high absorption coefficient in the region of λ<600 nm, the value of which increases with an increase in the content of Al_2O_3 nanoparticles. In addition, the graph shows the wavelength of the optical absorption edge, determined by the method of linear extrapolation of the steeply increasing section of the spectrum. The dependence of the absorption edge position on the concentration of Al_2O_3 nanoparticles is presented in Table 1. The optical absorption edge corresponds to the energy threshold of the interband transition and reflects the fundamental width of the band gap [24].

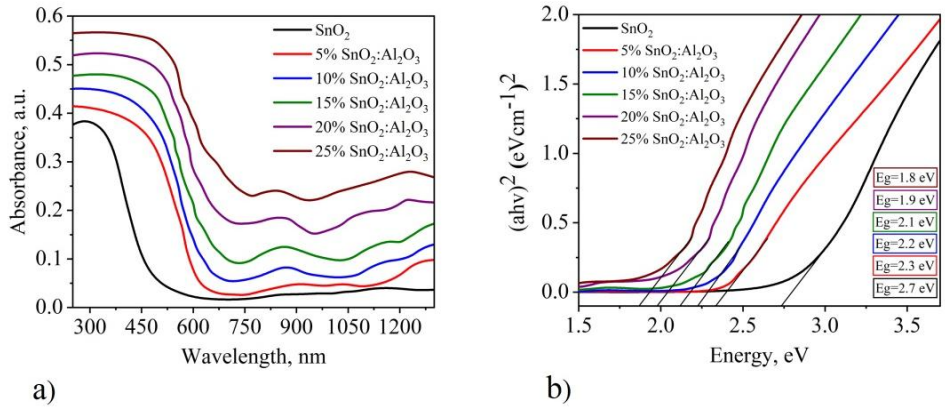

Figure 4. Absorption and Tauc plot of SnO_2 and SnO_2:Al_2O_3 (5 %, 10 %, 15 %, 20 %, 25 %)

With increasing concentration of Al_2O_3, a regular shift of the absorption edge to the region of longer wavelengths is observed, which indicates a change in the optical width of the forbidden material. In particular, for the SnO_2 film, the wavelength of the absorption edge is 320 nm, whereas for films with Al_2O_3 nano-

particles in concentrations of 5 %, 10 %, 15 %, 20 % and 25 %, this parameter increases to 419 nm, 451 nm, 482 nm, 498 nm and 506 nm.

Table 1

Optical parameters of SnO_2 and SnO_2:Al_2O_3 (5 %, 10 %, 15 %, 20 %, 25 %)

Samples	λ_{edge}, nm	D_λ, optical density	Optical band gap (eV)
SnO_2	320	0.37	2.83
5 % SnO_2:Al_2O_3	419	0.41	2.33
10 % SnO_2:Al_2O_3	451	0.44	2.24
15 % SnO_2:Al_2O_3	482	0.47	2.12
20 % SnO_2:Al_2O_3	498	0.51	1.98
25 % SnO_2:Al_2O_3	506	0.56	1.87

Figure 4*b* shows the dependence of the optical band gap on the concentration of Al_2O_3 nanoparticles in SnO_2 and SnO_2:Al_2O_3 thin films with a content of 5 %, 10 %, 15 %, 20 % and 25 %. The optical band gap values of the films were calculated using the Tauc plot method [25]. The change in the optical band gap allows characterizing the electrical properties of the material, since it is directly related to the energy difference between the valence band and the conduction band. According to the data presented in Table 1, an increase in the concentration of Al_2O_3 nanoparticles leads to a consistent decrease in the optical band gap: for the SnO_2 film it is 2.83 eV, while for the composite films it decreases to 1.87 eV with an increase in the concentration of Al_2O_3 nanoparticles. It should be noted that reducing the optical band gap improves the transition of electrons from the valence band to the conduction band, resulting in an increase in the conductivity of the material [26].

Photoelectrical characterizations

Figure 5 shows the current-voltage characteristics of polymer solar cells with the FTO/SnO_2:Al_2O_3/P3HT:PCBM/PEDOT:PSS/Ag structure with ETL based on SnO_2 with different contents of Al_2O_3 nanoparticles. The current-voltage characteristics parameters are given in Table 2. Upon photoexcitation of the photoactive P3HT:PCBM layer, an electron–hole pair is formed, which then disintegrates into free charge carriers at the SnO_2/P3HT:PCBM and P3HT:PCBM/PEDOT:PSS interface. As a result, electrons are injected into the ETL layer of SnO_2, and holes into the hole transport layer (HTL) of PEDOT:PSS (Fig. 5*b*). As a result of this process, a photocurrent will flow in the circuit under study. Al_2O_3 nanoparticles in the ETL serve to block the process of reverse electron transfer from SnO_2 to the PCBM acceptor. Addition of Al_2O_3 nanoparticles to a concentration of 15 % in the SnO_2 film promotes an increase in the short-circuit current density by 32 %. A further increase in the concentration of Al_2O_3 nanoparticles leads to a decrease in the short-circuit current density. The efficiency of the cell with SnO_2 was 1.9 %, while it increased to 2.8 % with the addition of Al_2O_3 nanoparticles at a concentration of 15 %.

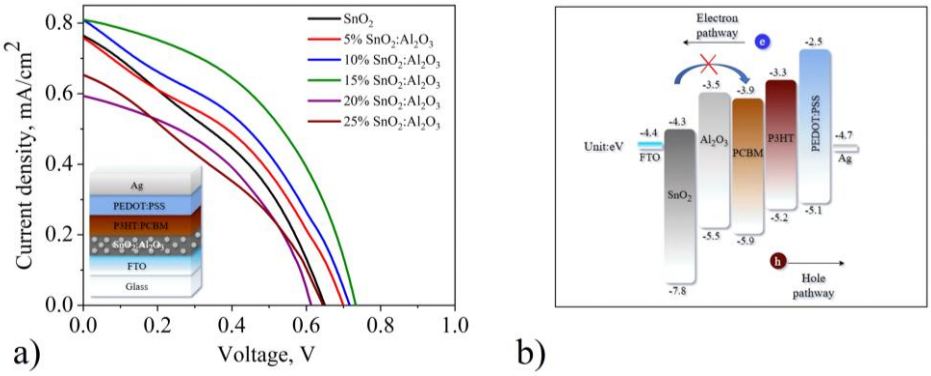

Figure 5. Current-voltage characteristics of SnO_2 and SnO_2:Al_2O_3 (5 %, 10 %, 15 %, 20 %, 25 %)

The increase in short-circuit current and cell efficiency with the addition of Al_2O_3 nanoparticles is associated with an increase in the concentration of free charge carriers in the composite film [27]. Additionally, Al_2O_3 nanoparticles reduce the number of surface defects, which decreases the probability of electron-hole recombination.

The decrease in efficiency with an increase in the content of Al_2O_3 nanoparticles above 15 % is obviously associated with the formation of structural and interphase defects that contribute to an increase in the recombination of charge carriers [28].

Table 2

Current-voltage parameters of SnO_2 and SnO_2:Al_2O_3 (5 %, 10 %, 15 %, 20 %, 25 %)

Samples	U_{oc} (V)	J_{sc} (mA/cm^2)	U_{max}(V)	J_{max} (mA/cm^2)	FF	PCE %
SnO_2	0.65±0.01	7.65±0.05	0.41±0.01	4.4±0.05	0.37	1.9±0.05
5 % SnO_2:Al_2O_3	0.7±0.01	7.55±0.05	0.43±0.01	4.6±0.05	0.38	2±0.05
10 % SnO_2:Al_2O_3	0.72±0.01	8 ±0.05	0.46±0.01	4.9±0.05	0.39	2.3±0.05
15 % SnO_2:Al_2O_3	0.73±0.01	8.1±0.05	0.51±0.01	5.4±0.05	0.46	2.8±0.05
20 % SnO_2:Al_2O_3	0.64±0.01	6.55±0.05	0.37±0.01	3.9±0.05	0.35	1.5±0.05
25 % SnO_2:Al_2O_3	0.61±0.01	5.9±0.05	0.38±0.01	4.1±0.05	0.43	1.6±0.05

To investigate the effect of Al_2O_3 nanoparticles on the electron transport of SnO_2 in polymer solar cells, electrical impedance spectra were measured (Fig. 6*a*).

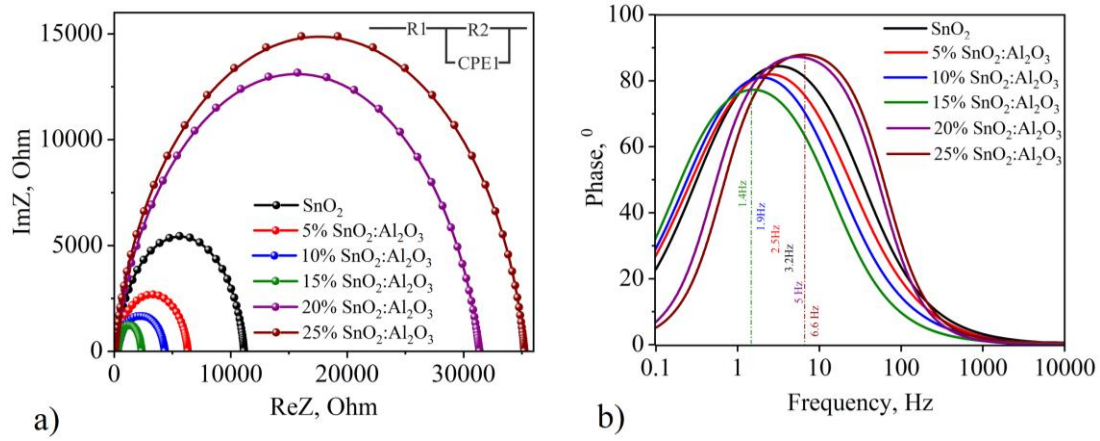

Figure 6. Impedance spectra and Bode plot SnO_2 and SnO_2:Al_2O_3 (5 %, 10 %, 15 %, 20 %, 25 %)

Figure 6(*a*) shows the impedance plots of the organic solar cells with the FTO/SnO_2:Al_2O_3/P3HT:PCBM/PEDOT:PSS/Ag structure. The electrical parameters were calculated based on the spectral data (Table 3) using the equivalent electrical circuit shown in the inset of Figure 6(*a*).

In this scheme, R_w denotes the equivalent resistance of the external electrodes (including R_{FTO}, $R_{SnO_2:Al_2O_3}$, PEDOT:PSS and Ag), and R_{tr} reflects the resistance associated with electron transfer at the interfaces between the P3HT:PCBM/SnO_2:Al_2O_3 and P3HT:PCBM/PEDOT:PSS layers. Table 3 shows the electrophysical parameters of the FTO/SnO_2:Al/P3HT:PCBM/PEDOT:PSS/Ag structure. The organic solar cell is a multilayer structure. Since the photoactive layer and the electrodes were deposited under the same conditions, the R_w value is almost the same in all cases. Its slight change with an increase in the Al_2O_3 concentration is associated with an insignificant change in the film thickness. Changes in the R_{tr} value indicate the influence of the P3HT:PCBM/ETL interface on the electron transfer process. A decrease in R_{tr} indicates an improvement in electron transport at the interface. As can be seen from Table 1, the cells with ETL with a concentration of Al_2O_3 nanoparticles of 15 % have the lowest resistance R_{tr}, which indicates the formation of a film with improved conductivity and a lower degree of defectiveness. However, with an increase in the concentration of Al_2O_3 nanoparticles above 15 %, an increase in recombination at the P3HT:PCBM/SnO_2:Al_2O_3 interface is observed, which is associated with the formation of structural and interphase defects.

The mobility of charge carriers is one of the most important electrotransport parameters of thin films. There are a number of methods for its experimental determination [29], but each of them is characterized by certain limitations and disadvantages [30]. In this work, we used the impedance spectroscopy method to determine the conditional mobility of charge carriers μ, in the studied samples described in detail in [31].

The diffusion coefficient *Dn* was determined by the following formula:

$$Dn = \frac{L^2}{\tau D}. \quad (1)$$

Where *L* is the film thickness, τD is the effective time of charge passage through the OSC. The value of the conditional hole mobility μ was determined by the formula:

$$\mu = \frac{e * Dn}{k_в * T}. \quad (2)$$

Where *e* is the electron charge, k_B is the Boltzmann constant, *T* is the temperature.

As can be seen from Table 1, the conditional electron mobility increases and has a maximum value for OSC with ETL based on SnO_2 with a concentration of Al_2O_3 nanoparticles equal to 15 %. The minimum value of the conditional electron mobility in OSC is observed for OSC with ETL based on SnO_2 with Al_2O_3 nanoparticles with a concentration of 25 %. Obviously, the observed decrease in the values of the conditional electron mobility in OSC with exceeding the concentration of Al_2O_3 nanoparticles of 15 % is explained by the different degrees of probability of electron scattering on defects formed at the P3HT:PCBM/SnO_2:Al_2O_3 interface.

Figure 6(*b*) shows the Bode plot analysis, which allows estimating the carrier lifetime in OSC [32]. As can be seen from Figure 6(*b*), the phase angle maximum for the cell (with 15 % Al_2O_3 nanoparticles in ETL) is shifted to lower frequencies compared to pure SnO_2-based ETL, indicating a longer carrier lifetime. This indicates a more effective suppression of charge recombination. Thus, the data clearly demonstrates the importance of the spatial separation of electron transport channels achieved by the incorporation of Al_2O_3 nanoparticles.

Table 3

Impedance parameters of SnO_2 and SnO_2:Al_2O_3 (5 %, 10 %, 15 %, 20 %, 25 %)

Samples	R_w, (Ohm)	R_{tr}, (Ohm)	*C*, (pF)	τ_D, (ps)	D_n, (cm^2, s^{-1})	μ, (cm^2V^{-1}, s^{-1})
SnO_2	68	11107	2.2517E-08	153	39.74	1.5
5 % SnO_2:Al_2O_3	72	6247	1.8231E-08	131	46.35	1.8
10 % SnO_2:Al_2O_3	81	4219	1.4762E-07	119	50.9	2
15 % SnO_2:Al_2O_3	87	2694	1.0923E-07	95	64	2.5
20 % SnO_2:Al_2O_3	64	31328	3.103E-08	198	30.64	1.2
25 % SnO_2:Al_2O_3	59	33105	3.719E-08	219	27.73	1.1

Thus, the conducted study demonstrates how the use of Al_2O_3 nanoparticles in ETL affects the efficiency of polymer solar cells. The obtained data can be applied in the development of optoelectronic devices, including integrated circuits, microelectronic optical systems, as well as organic photoconverters, sensors and light-emitting diodes (OLEDs).

Conclusions

Composite SnO_2 films with different contents of Al_2O_3 nanoparticles were obtained by the sol-gel method. The effect of Al_2O_3 nanoparticles on the surface morphology of the films was studied using scanning electron microscopy and atomic force microscopy. It is shown that the addition of Al_2O_3 nanoparticles to SnO_2 promotes the formation of a more uniform and smooth surface. This may be due to the improvement of film formation conditions and a decrease in grain size due to the introduction of Al_2O_3 nanoparticles, which affect the growth of crystals in the film. The results of measuring the absorption spectra showed that an increase in the concentration of Al_2O_3 nanoparticles in the structure leads to a gradual decrease in the width of the optical bandgap of the material from 2.33 eV to 1.87 eV. This decrease indicates a change in the electronic structure, probably associated with the formation of new energy sublevels resulting from the interaction of Al_2O_3 nanoparticles with the SnO_2matrix. Impedance spectroscopy revealed a reduction in recombination and an increase in charge carrier mobility at an Al_2O_3 nanoparticle concentration of 15 %, which contributes to the improvement of the material's transport properties. However, at high concentrations of Al_2O_3 nanoparticles (over 15 %), the opposite effect is observed — increased recombination and decreased mobility, which is associated with the formation of interphase defects that disrupt the continuity of the conductive paths. Photoelectric measurements showed that the maximum efficiency of solar cells was 2.5 % at

the optimal concentration of Al_2O_3. With a further increase in the content of Al_2O_3 nanoparticles (over 15 %), a decrease in efficiency is observed. This can be explained by an increase in the density of defects that impair the collection and transport of charges.

Funding

This research is funded by the Science Committee of the Ministry of Science and Higher Education of the Republic of Kazakhstan (Grant No. AP19679938).

References

1 Omura, K., Veluchamy, P., Tsuji, M., Nishio, T., & Murojono, D. (1999). Synthesis and Characterization of Nano-Crystalline Fluorine-Doped Tin Oxide Thin Films by Sol-Gel Method. *J. Electrochem. Soc., 146*, 2113. https://doi.org/10.1023/A:1025697322395

2 Laverty, S.J., Feng, H., & Maguire, P. (1997). Adhesion of Copper Electroplated to Thin Film Tin Oxide for Electrodes in Flat Panel Displays. *J. Electrochem. Soc., 144*, 2165; https://doi.org/10.1149/1.1837758

3 Tadeev, A.V., Delabouglise, G., & Labeau, M. (1998). Influence of Pd and Pt additives on the microstructural and electrical properties of SnO_2-based sensors. *Mater. Sci. Engg. B57*, 76; https://doi.org/10.1016/S0921-5107(98)00251-7

4 Chopra, K.L., Major, S., & Pandya, D.K. (1983). Transparent conductors-A status review. *Thin Solid Films, 102*, 1; https://doi.org/10.1016/0040-6090(83)90256-0

5 Dawar, A.L., & Joshi, J.C. (1984). Semiconducting transparent thin films: their properties and applications. *J Mater Sci., 19*, 1–23; https://doi.org/10.1007/BF02403106

6 Freeman, A.J., Poeppelmeier, K.R., Mason, T.O., Change, R.P.H., & Marks, T.J. (2000). Chemical and Thin-Film Strategies for New Transparent Conducting Oxides. *MRS Bull. 25*, 45; https://doi.org/10.1557/mrs2000.150

7 Ginley, D.S., & Bright, C. (2000). Transparent Conducting Oxides. *MRS Bull., 25*, 15–18; https://doi.org/10.1557/mrs2000.256

8 Rozati, S.M., & Akesteh, S. (2007). Influence of Air Flow Rate on Physical Properties of Zinc Oxide. *Mater. Charact., 58*(4), 319; http:// doi.org/10.1007/978-3-540-75997-3_270

9 Bohle, D.S., & Spina, C.J. (2007). The Relationship of Oxygen Binding and Peroxide Sites and the Fluorescent Properties of Zinc Oxide Semiconductor Nanocrystals. *J. Am. Chem. Soc., 129*(41), 12380; https://doi.org/10.1021/ja0747223

10 Fonoberov, V.A., Alim, K.A., Balandin, A.A., Xiu, F.X., & Liu, J.L. (2006). Photoluminescence investigation of the carrier recombination processes in ZnO quantum dots and nanocrystals. *Phys. Rev. B., 73*(16), 165317–20; https://doi.org/10.1103/PhysRevB.73.165317

11 Klenk, R. (2001). Characterisation and modelling of chalcopyrite solar cells. *Thin Solid Films, 387*(1-2), 135–140; https://doi.org/10.1016/S0040-6090(00)01736-3

12 Cowan, S.R., Schulz, P., Giordano, A.J., Garcia, A., Macleod, B.A., Marder, S.R., Kahn, A., Ginley D.S., Ratcliff E.L., & Olsen, D.C. (2014). Chemically Controlled Reversible and Irreversible Extraction Barriers Via Stable Interface Modification of Zinc Oxide Electron Collection Layer in Polycarbazolebased Organic Solar Cells. *Adv. Funct. Mater., 24*(29), 4671–4680; https://doi.org/10.1002/adfm.201400158

13 Wu, B., Wu, Zh., Yang, Q.Y., Zhu, F.R., Ng, T.W., Lee, C.S., Cheung, S.H. & So, S.K. (2016). Improvement of Charge Collection and Performance Reproducibility in Inverted Organic Solar Cells by Suppression of ZnOSubgap States. *ACS Appl. Mater. Inter., 8*(23), 14717–14724; https://doi.org/10.1021/acsami.6b03619

14 Xu, T., Tian, Zh., Elmi, O., Krzeminski, C., Robbe, O., Lambert, Y., Yakeda, D., Okada, E., Wei, B., & Stiévenard, D. (2017). Optical and electrical properties of nanostructured implanted silicon n+ -p junction passivated by atomic layer deposited Al_2O_3. *Physica E., 93*, 190; https://doi.org/10.1016/j.physe.2017.06.017

15 Wang, W.C., Lin, C.W., Chen, H.J., Chang, C.W., Huang, J.J., Yang, M.J., Tjahjono, B., Huang, J., Hsu, W.C., & Chen, M.J. (2013). Surface Passivation of Efficient Nanotextured Black Silicon Solar Cells Using Thermal Atomic Layer Deposition. *ACS Appl. Mater. Inter., 5*(19), 9752–9759; https://doi.org/10.1021/am402889k

16 Lee, H., Tachibana, T., Ikeno, N., Hashiguchi, H., Arafune, K., Yoshida, H., Satoh, S., & Chikyow, T. (2012). Interface engineering for the passivation of c-Si with O-3-based atomic layer deposited AlOx for solar cell application. *Appl. Phys. Lett., 100*(14), 253504; https://doi.org/10.1063/1.3701280

17 Dingemans, G., & Kessels, W. (2012). Status and prospects of Al_2O_3-based surface passivation schemes for silicon solar cells. *Journal of Vacuum Science & Technology A., 30*, 040802; https://doi.org/10.1116/1.4728205

18 Zhao, S.Y., Liu, X.K., Gu, W., Liang, X.Y., Ni, Z.Y., Tan, H., Huang, K., Yan, Y.C., Yu, X.G., Xu, M.C., Pi, X.D., & Yang, D.R. (2018). Al_2O_3-Interlayer-Enhanced Performance of All-Inorganic Silicon-QuantumDotNear-Infrared Light-Emitting Diodes. *IEEE Transactions on electron devices. 65*, 577; https://doi.org/10.1109/TED.2017.2782772

19 Poodt, P., Cameron, D.C., Dickey, E., George, S.M., Kuznetsov, V., Parsons, G.N., Roozeboom, F., Sundaram, G., & Vermeer, A.J. (2012). Spatial atomic layer deposition: A route towards further industrialization of atomic layer deposition. *Vac. Sci. Technol. A., 30*, 010802; https://doi.org/10.1116/1.3670745

20 Xu, C., Tamaki, J., Miura, N., & Yamazoe, N. (1991). Promotion of tin oxide gas sensor by aluminum doping. *Talanta, 38*, 1169; https://doi.org/10.1016/0039-9140(91)80239-V

21 Mohagheghi, M., & Saremi, M. (2004). Optical and Electrical Conductivity of SnO:Cu Nanoparticles. *J. Phys. D: Appl. Phys. 37*, 1248; https://doi.org/10.23851/mjs.v32i3.944

22 Chen, P., & Yin, X. (2017). Low temperature solution processed indium oxide thin films with reliable photoelectrochemical stability for efficient and stable planar perovskite solar cells, *J. Mater. Chem. A., 5* (20) 9641–9648; https://doi.org/10.1039/c7ta00183e

23 Marikkannan, M., Vishnukanthan, V., Vijayshankar, A., Mayandi, J., & Pearce, J.M. (2015). A novel synthesis of tin oxide thin films by the sol-gel process for optoelectronic applications. *AIP Advances, 5*, 027122; https://doi.org/10.1063/1.4909542

24 Qin, C., Kim, J.B., Gonome, H., & Lee, B.J. (2020). Absorption characteristics of nanoparticles with sharp edges for a direct-absorption solar collector. *Renew Energy, 145*, 21; https://doi.org/10.1016/j.renene.2019.05.133

25 Harynski, T., Olejnik, A., Grochowska, K., & Siuzdak, K., (2022). A facile method for Tauc exponent and corresponding electronic transitions determination in semiconductors directly from UV–Vis spectroscopy data. *Optical Materials. Vol. 127*, 112205; https://doi.org/10.1016/j.optmat.2022.112205

26 Kamarulzamanet. al. (2015). Band Gap Narrowing and Widening of ZnO Nanostructures and Doped Materials. *Nanoscale Research Letters, 10*, 346; https://doi.org/10.1186/s11671-015-1034-9

27 Gunasekar, K., Chakravarthi, N., Cho, W., Lee, J.W., Kim S.W., S.H., Kotov, Cha, N.A., & Jin, J.H. (2015). Optimization of polymer solar cells performance by incorporated scattering of ZnO nanoparticles with different particle geometry. *Synthetic Metals. Vol. 205*, 185–189; https://doi.org/10.1016/j.synthmet.2015.04.009

28 Kavanagh, S.R., Scanlon, D.O., & Walsh, A. (2022). Impact of metastable defect structures on carrier recombination in solar cells. Faraday discussions; https://doi.org/10.1039/D2FD00043A

29 Kar, A., Sain, S., Kundu, S., Bhattacharyya, A., Pradhan, S.K., & Patra, A. (2015). Influence of size and shape on the photo-catalytic properties of SnO_2 nanocrystals. *Chem. Phys. Chem., 16,* 1017–1025; https://doi.org/10.1002/cphc.201402864

30 Mahmoud, S.A., Alshomer, S., & Tarawnh, M.A. (2011). Structural and optical dispersion characterisation of sprayed nickel oxide thin films, *J. Mod. Phys. 2*, 1178–1186; https://doi.org/10.4236/jmp.2011.210147.

31 Rashad, M., Darwish, A.A., & Attia, A.A. (2017). Impact of film thickness on optical and electrical transport properties of noncrystalline GeSe1.4Sn0.6 films, *J. Non-Cryst. Solids, 470*, 1–7; https://doi.org/10.1016/j.jnoncrysol.2017.04.015.

32 JunSeo, Y., Arunachalam, M., Ahn, K.-S., & Hyung Kang, S. (2021). Integrating heteromixtured Cu_2O/CuO photocathode interface through a hydrogen treatment for photoelectrochemical hydrogen evolution reaction, Appl. Surf. Sci. 551, 149375; https://doi.org/10.1016/j.apsusc.2021.149375

Ә.Қ. Мұсабекова, А.К. Аймуханов, А.К. Зейниденов,
А.З. Зият, К.Т. Абдрахман, А.М. Алексеев

Al_2O_3 нанобөлшектерінің полимерлі күн элементіндегі электрондарды тасымалдауға әсері

Полимерлі күн элементтерінде SnO_2 негізінде алынған электрон тасымалдаушы қабатына (ETL) Al_2O_3 нанобөлшектерінің әсері зерттелді. Композиттік қабыршақтардың морфологиялық, оптикалық, электрофизикалық және фотоэлектрлік қасиеттерінің кешенді зерттеулері жүргізілді. SnO_2 қабыршақтарына Al_2O_3 нанобөлшектерін қосу арқылы композиттік қабыршақтар бетінің кедір-бұдырлығының төмендеуі анықталды. Жұтылу спектрлері арқылы SnO_2 қабыршақтарында Al_2O_3 нанобөлшектерінің концентрациясын арттыру оптикалық тыйым салу аймағы енінің азаюына алып келетіні айқындалды. Импеданс спектрлерін талдау арқылы SnO_2 кабыршақтарында Al_2O_3 нанобөлшектерінің электрондарды тасымалдаудың жоғары сипаттамалары анықталатын критикалық концентрациясы бар екені көрсетілді. Зерттелетін композиттік қабыршақтардың Al_2O_3 нанобөлшектерінің жоғары концентрациясында (15 %-дан жоғары) электрондардың қозғалғыштығының төмендеуі және рекомбинациясының жоғарылауы байқалады. Фотоэлектрлік өлшеулер арқылы ең жоғары пайдалы әсер коэффициенті (ПӘК) 2,8 % полимерлі күн элементтерінің Al_2O_3 нанобөлшектерінің оңтайлы концентрациясы 15 % екенін көрсетті. Al_2O_3 нанобөлшектерінің концентрациясының одан әрі артуы полимерлі күн элементтерінің ПӘК-нің төмендеуіне әкеледі. Al_2O_3 нанобөлшектеріндегі локализацияланған теріс зарядтар жергілікті электр өрісін тудыратындықтан, олар SnO_2 ETL-да негізгі емес заряд тасымалдаушылардың рекомбинациясын экрандайды. Бұл құрылғылардағы токтың ағып кетуін тежейді. Сондықтан SnO_2:Al_2O_3 қабыршақтарындағы зарядты тасымалдау механизмін зерттеу және олардың полимерлі күн элементтерінде қолдану потенциалын бағалау маңызды.

Кілт сөздер: SnO_2, Al_2O_3, морфология, жұтылу, тыйым салу аймағының ені, Боде графигі, импеданс, вольт-амперлік сипаттамалар

А.К. Мусабекова, А.К. Аймуханов, А.К. Зейниденов,
А.К. Зият, К.Т. Абдрахман, А.М. Алексеев

Влияние наночастиц Al_2O_3 на электронный транспорт в полимерном солнечном элементе

Изучено влияние наночастиц Al_2O_3 на электронный транспорт (ETL) на основе SnO_2 в полимерных солнечных элементах. Проведен комплексный исследования морфологических, оптических и электрофизических и фотоэлектрических свойств композитных пленок. Было выявлено, что допирование наночастицами Al_2O_3 пленок SnO_2 приводит к уменьшению шероховатости поверхности композитных пленок. По данным спектров поглощения показано, что увеличение концентрации наночастиц Al_2O_3 в пленках SnO_2 приводит к уменьшению оптической ширины запрещённой зоны. Анализ спектров импеданса показал, что существует критическая концентрация наночастиц Al_2O_3 при которой наблюдается максимальноеулучшение электротранспортных характеристик пленок SnO_2. При высоких концентрациях Al_2O_3 (свыше 15 %) наблюдается снижение подвижности электронов и усиление рекомбинации в исследуемой композитной пленке. Фотоэлектрические измерения продемонстрировали, что наибольший коэффициент полезного действия (КПД) 2,8 % полимерных солнечных элементов достигается при оптимальной концентрации наночастиц Al_2O_3 равной 15 %. Дальнейшее увеличение содержания наночастиц Al_2O_3 приводит к снижению КПД полимерных солнечных элементов. Так как локализованные отрицательные заряды в наночастицах Al_2O_3 создают локальное электрическое поле, то они экранируют рекомбинацию неосновных носителей заряда в ETLSnO_2. Это подавляет утечку тока в устройствах. Поэтому важно исследовать механизм переноса зарядов в плёнках SnO_2:Al_2O_3 и оценить их потенциал применения в полимерных солнечных элементах.

Ключевые слова: SnO_2, Al_2O_3, морфология, поглощение, ширина запрещенной зоны, график Боде, импеданс, вольт-амперные характеристики

Information about the authors

Mussabekova, Assel (*contact person*) — PhD student, Buketov University, Karaganda 100028, Kazakhstan; e-mail: assel50193@gmail.com; Scopus Author ID: 58429663700, ORCID ID: https://orcid.org/0000-0003-3452-4622

Aimukhanov, Aitbek — Candidate of Physical and Mathematical Sciences, Professor, Buketov University, Karaganda 100028, Kazakhstan, e-mail: a_k_aitbek@mail.ru; Scopus Author ID: 58493008700, ORCID ID: https://orcid.org/0000-0002-4384-5164

Zeinidenov, Assylbek — PhD, Professor, Buketov University, Karaganda 100028, Kazakhstan, e-mail: asyl-zeinidenov@mail.ru; Scopus Author ID: 56386144000; ORCID ID: https://orcid.org/0000-0001-9232-8406

Ziyat, Aizhuldyz — Master of Educational Sciences, Buketov University, Karaganda 100028, Kazakhstan, e-mail: aizhuldyz_12@mail.ru; ORCID ID: https://orcid.org/0009-0005-3310-9058

Abdrakhman, Kelbet — Master of Technical Sciences, Buketov University, Karaganda 100028, Kazakhstan, e-mail: kelbet.abdraxman@mail.ru

Alexeev, Alexandr — Candidate of Physical and Mathematical Sciences, Kazan Federal University, Kazan, Russia, e-mail: alalrus@mail.ru; Researcher ID: A-8526-2012, ORCID ID: https://orcid.org/0000-0002-2800-6047